

Demonstration of WDM OSNR Performance Monitoring and Operating Guidelines for Pol-Muxed 200-Gbit/s 16-QAM and 100-Gbit/s QPSK Data Channels

M. R. Chitgarha¹, S. Khaleghi¹, W. Daab¹, M. Ziyadi¹, A. Mohajerin-Ariaei¹, D. Rogawski¹, M. Tur²,
J. D. Touch³, V. Vusirikala⁴, W. Zhao⁴, A. E. Willner¹

1) Ming Hsieh Department of Electrical Engineering, University of Southern California, 3740 McClintock Ave, Los Angeles, CA 90089, USA

2) School of Electrical Engineering, Tel Aviv University, Ramat Aviv 69978, Israel

3) Information Sciences Institute, University of Southern California, 4676 Admiralty Way, Marina del Rey, CA, 90292, USA

4) Google Inc., 1600 Amphitheatre Parkway, Mountain View, CA 94043, USA
chitgarh@usc.edu

Abstract: We demonstrate an optical-signal-to-noise-ratio (OSNR) monitoring scheme of 200-Gbit/s PM-16QAM and 100-Gbit/s QPSK signals using Mach-Zehnder delay-line-interferometer with <0.5 dB error for signals with up to 22 dB actual OSNR. We have also shown usability of this scheme by varying different parameters and have determined design guidelines to achieve a desired level of accuracy.

OCIS codes: (060.2360) Fiber optics links and subsystems; (060.4257) Networks, network survivability

1. Introduction

Optical performance monitoring has gained much interest for helping maintain proper system operation in optical communication networks. One of the most basic parameters to measure at various points around a network is the optical signal-to-noise ratio (OSNR), and there have been several approaches that have been reported [1-11]. In addition to the main point that the monitor should specifically measure the signal and in-channel-band noise, there are several desirable features for an OSNR monitor that include the following points. First, the monitor should be potentially cost effective (i.e., integratable with minimal complexity) so that it can be deployed ubiquitously around the network to help diagnose and locate problems. Importantly, although coherent receivers can recover the OSNR, such receivers tend to be costly and the OSNR information may be needed at many different locations not specifically at the coherent receiver itself. Second, the monitor should accommodate different types of data modulation formats and bit rates with a minimal amount of in-situ monitor tuning; these modulation formats should probably include various forms related to polarization multiplexing as well as higher-order formats such as quadrature-phase-shift-keying (QPSK) and quadrature amplitude modulation (QAM) [11]. Third, the monitors should be useful for deployment by having well-defined operating design parameters and reasonable accuracy [2].

One type of OSNR monitor that holds promise for achieving many of the desired characteristics is the Mach-Zehnder-based delay-line interferometer (DLI) [2,8]. The DLI-based OSNR monitor measures the optical power of the constructive and destructive output ports using simple low-speed photodiodes in order to determine the signal and noise powers. The signal is coherent and experiences constructive and destructive interference in the DLI, whereas the in-band noise is typically noncoherent and experiences simple power splitting from the DLI. Previous results using this type of monitor include single-WDM-channel 40-Gbit/s BPSK data in a non-pol-muxed system [8]. Laudable goals for the ultimate usability of this DLI monitor would be demonstrating its viability to measure high-bit-rate pol-muxed QPSK and QAM data in a WDM system, as well as determining important design guidelines and level of accuracy for practical deployment.

In this paper, we examine, provide design guidelines and demonstrate an OSNR performance monitor for 200 Gbit/s pol-muxed 16-QAM and 100 Gbit/s pol-muxed QPSK in both single and WDM data channels. Our OSNR monitoring scheme is capable of achieving <0.5 dB error for signals with <22 dB actual OSNR. We also examine different parameters to determine the design guidelines for a desired level of OSNR monitor accuracy in a network. The performance is assessed by measuring the OSNR error at wide range of delay, phase and filter parameters.

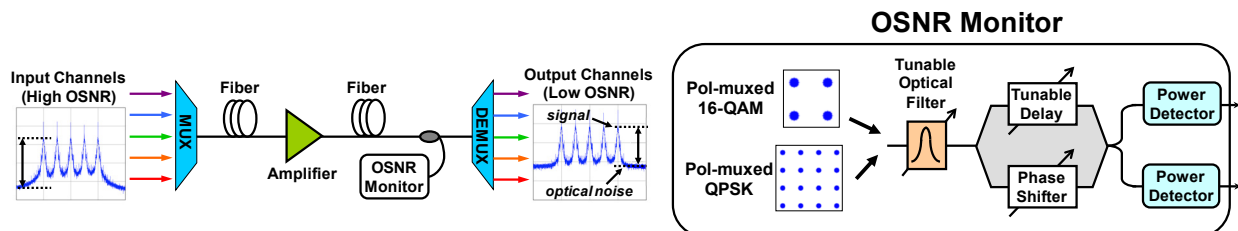


Fig. 1. Conceptual block diagram of the OSNR monitor for WDM channels using a delay-line-interferometer.

2. Concept

The conceptual block diagram of OSNR monitor scheme is shown in Fig. 1. The monitor consists of a tunable optical filter to extract a desired channel from a WDM system and a DLI followed by two power detectors to measure DLI output powers. This optical filter along with all cascaded filters in the optical link can be seen as an effective bandpass filter (BPF) centered at λ_0 and with bandwidth of Δf . The DLI with a delay T on one of its arm is indeed a finite impulse response filter with FSR of $1/T$ and is polarization insensitive. When only signal is sent through the monitor (i.e., OSNR is very high), we define the ratio between the powers of the constructive and the destructive ports as α . Similarly, we define β as the noise distribution ratio for the case when only ASE noise is transmitted. Because optical filters are linear systems, the net power distribution between DLI ports is the summation of power distribution of signal and noise between DLI output ports individually. According to the superposition property, $P_{Dest} = \frac{1}{\alpha+1}P_{Sig} + \frac{1}{\beta+1}P_N$ and $P_{Const} = \frac{\alpha}{\alpha+1}P_{Sig} + \frac{\beta}{\beta+1}P_N$, in which P_{Const} , P_{Dest} , P_{Sig} and P_N are the measured power at the constructive port, measured power at the destructive port, actual signal power and actual noise power, respectively. Thus, by solving this system of linear equations, one can obtain the OSNR from the measured DLI powers $OSNR = \frac{P_{Sig}}{P_N} = \frac{(\alpha+1)(P_{Const}-\beta P_{Dest})}{(\beta+1)(\alpha P_{Dest}-P_{Const})}$. The error of this calculated OSNR, therefore, depends on the measurement accuracy of P_{Const} , P_{Dest} , α and β . Both α and β depend on the frequency response of effective BPF as well as the FSR of the DLI. This measurement accuracy is determined by the resolution of power meters, stability of the DLI's parameters (i.e., phase and delay) and stability of the effective BPF frequency response (i.e., center frequency, bandwidth, and shape).

3. Experimental Setup

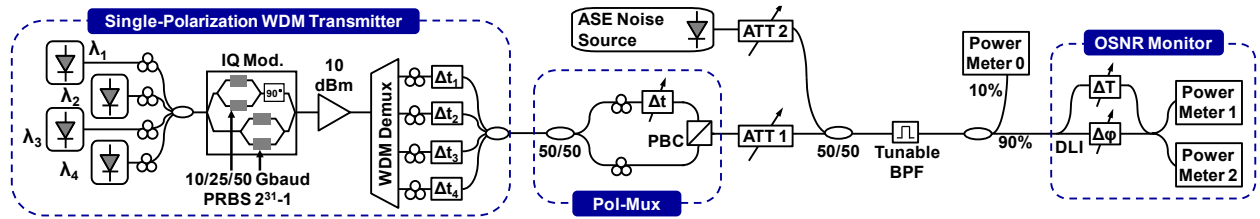


Fig. 2. Experimental setup for simultaneous OSNR monitoring of polarization multiplexed signals.

As depicted in Fig. 2, to create a 4-channel WDM system, four lasers (50-GHz ITU grid, around 1550 nm) are sent into an IQ modulator that is driven by $2^{31}-1$ pseudo-random bit sequence (PRBS) data at variable baud rates (10/25/50 GHz). The single-polarization signal is then split to half, delayed and combined in a polarization beam combiner (PBC) to emulate pol-mux. An ASE broadband noise source is coupled with the signal(s). Attenuators (ATT) are used on the signals and the noise path to vary OSNR. A WDM channel is then selected using a tunable Gaussian BPF and sent to the OSNR monitor (a tunable DLI and power meters). The 10% tap is used after the filter to measure actual signal and noise powers (i.e., actual OSNR).

4. Results and Design Guidelines

The proposed OSNR monitor has four design parameters: (a) the delay of DLI (ΔT), (b) maximum DLI phase detuning ($\Delta\phi$), (c) filter bandwidth (Δf) and (d) filter center frequency. In order to realize accurate OSNR monitoring in an optical network, the following design rules and guidelines need to be considered for any optical network. First, for monitoring a specific channel, the center frequency of the BPF filter needs to be tuned to the center of that channel. The filter bandwidth cannot be significantly wider than the effective bandwidth of each channel to minimize the negative effects of the leaked neighboring channels in the WDM systems [9]. Very narrowband filter, on the other hand, can change the actual OSNR of the signal and increases the error. Second, the trade-off in choosing the DLI delay value lies in the fact that smaller delays can often increase the accuracy of the OSNR monitor but they are more sensitive to the DLI phase fluctuations. Here, since we monitored multiple 50-GHz-spaced WDM channels at 25 Gbaud, the bandwidth of the filter is 0.3 nm (equivalent to at least three consecutive filters with 50 GHz bandwidth). Two types of filter (Gaussian and Lorentzian) are studied. In Fig. 3, the accuracy of the proposed scheme for OSNR monitoring is assessed for DLIs with different delays for three levels of OSNR: low (5 dB), medium (15 dB) and high (20 dB), and a Lorentzian filter shape. As simulations show, the error level increases for higher delays. It is worth mentioning that in each experimental measurement, in order to minimize the DLI phase drifting effect, the DLI voltage is tuned so that the power ratio between constructive and destructive ports is maximized. In Fig. 4, the actual OSNR and the filter bandwidth are fixed at 20 dB and 0.3 nm, respectively, and the OSNR measurement error is calculated based on both simulations and experiment for different

DLI phases. In Fig. 5, an error margin of 18 degrees for DLI phase drifting is assumed and the total OSNR measurement error is depicted for different DLI delay values. This phase fluctuation can be the result of temperature changes. We can conclude from simulations and experiments that the optimum value for DLI delay is 7 ps (17.5% of the symbol time) for 100-Gbit/s PM-QPSK signals, with either Lorentzian or Gaussian filter shapes. For this value, the OSNR monitor achieves < 0.5 dB measurement accuracy. The rest of the experiments have also been performed using a 7-ps DLI.

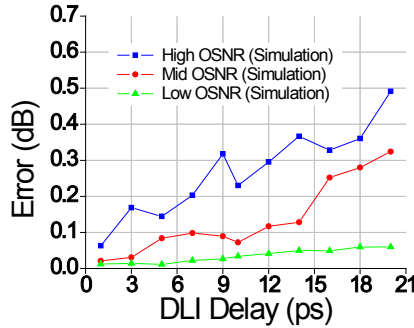


Fig. 3. Simulated measurement error vs. DLI delay for low (5 dB), medium (15 dB) and high (20 dB) OSNR, 100-Gbit/s PM-QPSK.

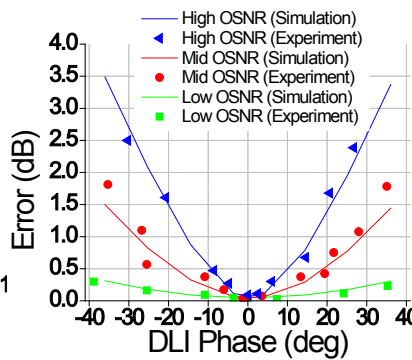


Fig. 4. Measurement error vs. DLI phase, simulation and experiment results for low (5 dB), medium (15 dB) and high (20 dB) OSNR, 100-Gbit/s PM-QPSK.

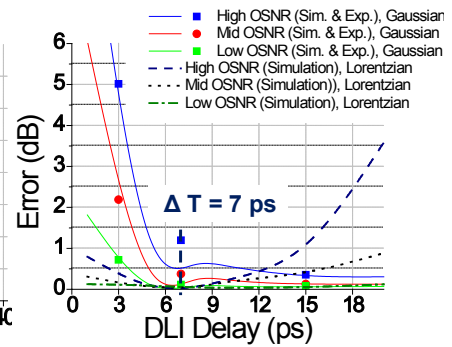


Fig. 5. Figure of merit (combination of phase instability and measurement error) vs. DLI delay, simulation and experiment results for low, medium and high OSNR, 100-Gbit/s PM-QPSK.

Fig. 6 depicts the accuracy of OSNR measurement for four WDM channels. For OSNR values of <22 dB, the OSNR monitor achieves <0.5 dB accuracy. It is worth noting that high accuracy in OSNR measurement is more important for lower (<20 dB) OSNR values, because the signal quality can become marginal for lower OSNRs. In Fig. 7, single channel at 1550.52 nm is modulated using BPSK, QPSK and 16-QAM formats at 25 Gbaud. The OSNR is measured with <0.5 dB error for OSNR values of <20 dB. Therefore, the same systems can also work for various modulation formats with the same baud rate. Fig. 8 shows measurement accuracy for QPSK signal with various baud rates (10, 25, and 50-Gbaud). For each baud rate, the filter bandwidth is changed accordingly. Again, <0.5 dB measurement error is observed for various bit-rates. We thus propose the following general design guidelines for the monitor: (a) choosing a sharp filter (with, e.g., Gaussian profile) before the DLI increases accuracy, (b) for the environment in which the monitor will be used at, determine how much DLI phase variations could happen, (c) use this to estimate an OSNR margin and create a figure-of-merit curve, (d) select the optimum delay for the DLI, and (e) pick power meter resolutions that meet the desired OSNR monitor accuracy.

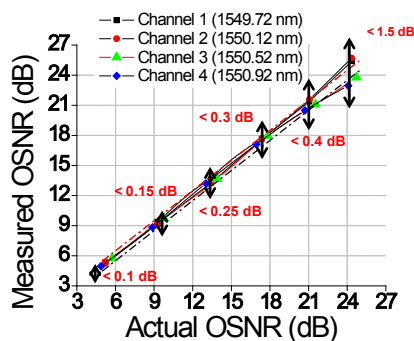


Fig. 6. Measured vs. actual OSNR for four 25-Gbaud PM-QPSK WDM channels and average error.

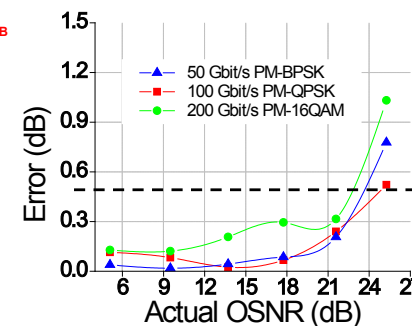


Fig. 7. Measurement error vs. actual OSNR for different modulation formats at same baud rate of 25-Gbaud.

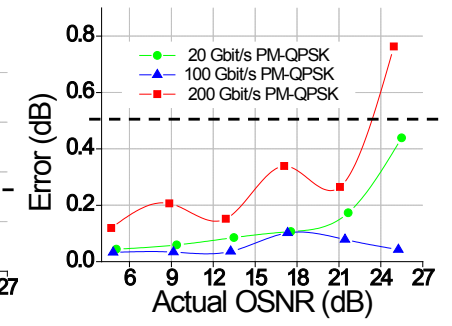


Fig. 8. Measurement error vs. actual OSNR for different baud rates and same modulation format PM-QPSK.

Acknowledgements

The authors would like to thank the support of Google and NSF CIAN.

5. References

[1] J. H. Lee, et al., J. Lightwave Technol. 24(11), (2006)
 [2] L.-S. Yan, et al., J. of Lightwave Technol. 23, 3290, (2005)
 [3] E. Flood, et al., Photon. Technol. Lett., 24(11), (2012)
 [4] J. Schröder, et al., J. of Lightwave Technol., 29(10), (2011)
 [5] F. N. Khan, et al., IEEE Photon. J., 4(5), (2012)
 [6] H. Y. Choi, et al., OFC, paper JThA16, (2010)
 [7] B. Kozicki, et al., Opt. Exp., 16, (2008)
 [8] X. Liu, et al., IEEE Photon. Technol. Lett. 19(15), (2007)
 [9] A. J. Zilkie, OFC, paper JThA12, (2009)
 [10] Z. Dong, et al., Opt. Express 20, 19520-19534 (2012)